[10]K. Kumar, Phys. Letters 29B, 25 (1969).
[11]R. J. Pryor and J. X. Saladin, Phys. Rev. 1, 1573 (1970).
[12]J. Eichler, Phys. Rev. B133, 1162 (1964).
[13]We did not use the formulation given in the review article of J. deBoer and J. Eichler, in *Advances in Nuclear Physics*, edited by M. Baranger and E. Vogt (Plenum Press, 1968), Vol. 1, since it contains some misprints.
[14]deBoer and Eichler (Ref. 13).
[15]A. C. Douglas and N. McDonald, Phys. Letters 24B, 447 (1967).
[16]H. S. Gertzman, D. Cline, H. E. Gove, and P. M. S. Lesser, Nucl. Phys. A151, 282 (1971).
[17]G. Engler, Phys. Rev. C 1, 734 (1970).
[18]R. G. Stockstad and I. Hall, Nucl. Phys. A99, 506 (1967).
[19]D. Cline, P. Jennens, C. W. Towsley, and H. S. Gertzmann, Bull. Am. Phys. Soc. II, 16, 1156 (1971).
[20]M. A. J. Mariscotti, G. Scharff-Goldhaber, and B. Buck, Phys. Rev. 178, 1864 (1969).
[21]A. S. Davydov and A. A. Chaban, Nucl. Phys. 20, 499 (1960).
[22]T. Tamura and T. Udagawa, Phys. Rev. 150, 783 (1966).

PHYSICAL REVIEW C VOLUME 6, NUMBER 3 SEPTEMBER 1972

Prompt Gamma Rays Emitted in the Thermal-Neutron-Induced Fission of $^{235}U^{\dagger}$

Frances Pleasonton, Robert L. Ferguson, and H. W. Schmitt
Oak Ridge National Laboratory, Oak Ridge, Tennessee 37830
(Received 20 March 1972)

The average number and average energy of γ rays emitted within ~5 nsec after fission have been determined as functions of fragment mass and as functions of fragment mass and total kinetic energy in two-dimensional representations. In a four-parameter experiment, energies of coincident pairs of fission fragments were measured with surface-barrier detectors and γ-ray energies were measured with a large NaI(Tl) detector, which was located 89 cm from a thin ^{235}U target and positioned coaxially with the fragment detectors. The time difference between detection of a fission fragment and a γ ray was measured to allow time-of-flight discrimination against fission neutrons. The γ-ray data were analyzed with a "weighting method" proposed by Maier-Leibnitz to deduce average numbers and energies of γ rays from measured pulse heights. The Doppler shift in the laboratory angular distribution of γ emission was utilized to obtain the number and energy of γ rays as functions of single fragment mass. The results, for both average number and average energy as functions of single fragment mass, are characterized by a sawtooth behavior similar to that which is well known for neutron emission. The over-all average number and energy of γ rays emitted per fission were found to be 6.51 ± 0.3 and 6.43 ± 0.3 MeV, respectively, giving an average photon energy of 0.99 ± 0.07 MeV.

INTRODUCTION

The present work has been undertaken to study in detail the average number and average energy of γ rays emitted in the thermal-neutron-induced fission of ^{235}U, as functions of fragment mass and total kinetic energy. The experiment is a four-parameter experiment in which, for each event, the kinetic energies of both fragments, the amplitude of the γ-ray pulse, and the time between the fragment pulse and γ-ray pulse were recorded. The time measurement was incorporated so that contributions from delayed γ rays and neutrons could be minimized. Careful calibrations and determination of the γ-ray spectrometer's response matrix allowed absolute energies and numbers to be obtained.

In this paper we describe the experiment and data analysis in some detail and include a derivation and discussion of the method, certain aspects of which may have been unclear in an earlier report.[1] Results for ^{235}U thermal-neutron fission are given, together with a qualitative discussion of them. Experiments on other low-excitation fission cases are in progress; a future paper will present those results together with a more complete interpretation of all of the results.

γ-ray emission in fission is studied to obtain spectroscopic data for the fragments formed, to obtain information about the angular momentum with which the fragments are formed, and to determine the number and energy of γ rays for fission energy-balance considerations or for nuclear applications.

Generally, two different but complementary techniques are used. In the spectroscopic experiments, a high-resolution γ-ray detector (e.g., a lithium-drifted germanium detector) measures γ-ray ener-

gies as accurately as possible and appropriate fragment-identification methods are used. In experiments to determine the average number, the average energy, or the angular distribution of γ rays emitted in fission, either with or without fragment identification, a lower-resolution higher-efficiency detector with a known response function may be used.

The spectroscopic experiments provide information about the nuclear-structure properties and the angular momenta of the nuclei formed as fission fragments. A number of studies of this type have been carried out on the spontaneous fission of ^{252}Cf, such as the recent experiments of John, Wesolowski, and Guy[2] on delayed γ rays (to 2 μsec) and those of Cheifetz *et al.*[3] and of Wilhelmy *et al.*[4,5] on prompt γ rays (<5 nsec). Prompt γ rays (~1 nsec) emitted in the thermal-neutron-induced fission of ^{235}U have been studied recently by Horsch[6,7] in high-resolution experiments making use of the Doppler shift in γ-ray energy.

Experiments to determine the average number or energy of γ rays emitted in fission, without fragment identification, have been carried out by a large number of experimenters; most recently those of Peelle and Maienschein[8] and Verbinsky and Sund[9] have improved the accuracy of the overall averages for ^{235}U thermal-neutron fission. Experiments which include correlations of γ rays with fission fragments have in general provided relative values of average γ-ray number or energy; these include, for example, the works of Maier-Leibnitz, Schmitt, and Armbruster[1] (whose experiment is the forerunner of this work), Albinsson and Lindow,[10] Albinsson,[11,12] and Armbruster, Labus, and Reichelt[13] for ^{235}U thermal-neutron fission. A recent experiment of Nifenecker *et al.*[14] on ^{252}Cf spontaneous fission included both fragment and neutron correlations, and was calibrated so that absolute average γ-ray numbers and energies could be obtained. Experiments of this type are important in determining the total energy balance for fission and in obtaining information about the average angular momenta of the fragments formed in fission.

BASIC METHOD

Let the angular distribution of γ rays from a particular fission fragment be $W(\theta)$ in the laboratory system and $W_0(\theta)$ in the fragment center-of-mass system, where $\theta=0$ is the direction of fragment flight. Note that the relation

$$W_0(\theta)=W_0(\theta+\pi) \tag{1}$$

holds, independent of the orientation of fragment spin with respect to the direction of the fragment. In contrast, $W(\theta)\neq W(\theta+\pi)$. We may define an anisotropy α_N in the laboratory system and give its value as follows:

$$\alpha_N \equiv \frac{W(\theta)-W(\theta+\pi)}{W(\theta)+W(\theta+\pi)} = 2\beta\cos\theta + f(\beta^2), \tag{2}$$

where $\beta=v/c$, i.e., the ratio of fragment velocity to the velocity of light, and where $f(\beta^2)$ represents higher-order terms in β.

Similarly, the total energy emitted per unit solid angle in the laboratory system shows an anisotropy

$$\alpha_E \equiv 3\beta\cos\theta + f(\beta^2). \tag{3}$$

Thus, maximum anisotropy for both number (subscript N) and energy (subscript E) occurs for $\theta=0$ (or π), an observation which is the basis for our choice of an experimental arrangement in which the γ-ray and fission-fragment detectors are aligned coaxially.

To determine the average number of γ rays emitted from single fission fragments, we proceed as follows:

The number of counts $n_{\gamma M}$ observed in the γ detector when a fragment of mass M is incident on detector No. 1 and a fragment of mass $A-M$ is incident on detector No. 2 (see Fig. 1) is:

$$n_{\gamma M} = p_\gamma n_M [\omega_M(1+2\beta_M) + \omega_{A-M}(1-2\beta_{A-M})], \tag{4}$$

where:

n_M (or n_{A-M}) is the total number of fissions for which fragments of mass M (or $A-M$) are incident on detector No. 1 and their complements of mass $A-M$ (or M) on detector No. 2.

β_M (or β_{A-M}) is the ratio of the velocity of a fragment of mass M (or $A-M$) to the velocity of light.

p_γ is the probability of detecting a γ ray (weighted average over the spectrum).

ω_M (or ω_{A-M}) is the average number of γ rays emitted from a fragment mass M (or $A-M$).

Similarly, when fragments of mass $A-M$ are incident on detector No. 1 and fragments of mass M are incident on detector No. 2, we observe a number of γ counts $n_{\gamma(A-M)}$ given by

$$n_{\gamma(A-M)} = p_\gamma n_{A-M} [\omega_M(1-2\beta_M) + \omega_{A-M}(1+2\beta_{A-M})]. \tag{5}$$

In Eqs. (4) and (5), the quantities n_M, n_{A-M}, β_M, β_{A-M} are determined from a separate, binary (fragment-fragment) coincidence experiment. The quantity p_γ is determined from the response matrix for our NaI(Tl) spectrometer by a method, originated by Maier-Leibnitz,[15] for obtaining a weighted average over a spectrum. The usual factors for solid angle, transmission and scattering in absorbing materials, and the total intrinsic efficiency of the NaI(Tl) crystal are included in p_γ.

The quantities ω_M and ω_{A-M} constitute the results we are seeking.

If we substitute $N(M) \equiv n_{\gamma M}/p_\gamma$ and $N(A-M) \equiv n_{\gamma(A-M)}/p_\gamma$ in Eqs. (4) and (5), and then add and subtract the equations, we obtain

$$\frac{N(M)}{n_M} + \frac{N(A-M)}{n_{A-M}} = 2\omega_M + 2\omega_{A-M} \tag{6}$$

and

$$\frac{N(M)}{n_M} - \frac{N(A-M)}{n_{A-M}} = 4\beta_M \omega_M - 4\beta_{A-M}\omega_{A-M}. \tag{7}$$

Simultaneous solution of these equations, together with use of conservation of momentum written in the form $(A-M)/M = \beta_M/\beta_{A-M}$, yields the average number of γ rays ω_M emitted from fragments of mass M:

$$\omega_M = \frac{M}{2n_M A}\{N(M) + (n_M/n_{A-M})N(A-M) + [N(M) - (n_M/n_{A-M})N(A-M)]/2\beta_{A-M}\}. \tag{8}$$

A similar expression can be written for ω_{A-M}.

For a pair of complementary fragments, the average total number of γ rays emitted per fission is given by $\omega_0 = \omega_M + \omega_{A-M}$. From Eq. (6) we obtain

$$\omega_0 = \frac{1}{2n_M}[N(M) + (n_M/n_{A-M})N(A-M)]. \tag{9}$$

In an ideal binary experiment we should obtain a perfectly symmetric mass distribution with equal yields of complementary fragments. In that case $n_M = n_{A-M}$, and Eqs. (8) and (9) simplify: Equation (8) becomes

$$\omega_M = \frac{M}{2n_M A}\left\{N(M) + N(A-M) + \frac{1}{2\beta_{A-M}}[N(M) - N(A-M)]\right\}, \tag{10}$$

and Eq. (9) becomes

$$\omega_0 = [N(M) + N(A-M)]/2n_M. \tag{11}$$

These equations will give the average energy (instead of number) of the γ rays if the factor 2 is replaced by 3 as the coefficient of the β's, and if values of p_γ that have been weighted according to the energies of the γ rays are used.

Appendixes I and II give detailed descriptions of the construction of the response matrix for our γ-ray spectrometer and the method of determining the p_γ's from it.

EXPERIMENT

The experiment was conducted at the Oak Ridge research reactor using a conventionally collimated neutron beam with a flux of $\gtrsim 10^8$ thermal neutrons $cm^{-2}\,sec^{-1}$. A 1-cm-diam target was prepared by vacuum evaporation of a thin deposit (~30 $\mu g\,cm^{-2}$) of $^{235}U_3O_8$ onto a thin carbon film (<2 MeV thick for fission fragments) which spanned an aperture of 2.4 cm in an Al frame. The fissile material contained 99.44% of ^{235}U, 0.0001% of ^{233}U, and a total of 0.56% of even uranium isotopes. The fission fragments were detected by silicon surface-barrier detectors and the γ rays by a NaI(Tl) spectrometer.

As shown in Fig. 1, the plane of the target was set at an angle of 45° with respect to the beam axis and to the faces of the two fragment detectors, with the fissile material facing detector No. 2. The detectors and target were mounted coaxially and were viewed, on axis, by the NaI(Tl) crystal (5 in. diam × 4 in. thick) at a distance of 89 cm from the target center. The crystal was mounted on a type 58-AVP photomultiplier tube.

The "near" detector (No. 1) was 600 mm^2 in area and was supported in a "transmission" mount at a distance of ~3.5 cm from the neutron-beam axis; it was protected from "edge effects" by a thin Mylar collimator (0.010 in.) with an aperture of ~$\frac{7}{8}$ in. diam. Its position and type of mounting were chosen to minimize attenuation and scattering of fission γ rays detected by the NaI(Tl) crystal. The "far" detector (No. 2) was smaller in area (400 mm^2), with its useful portion restricted to ~200 mm^2 by a similar collimator whose inside diameter was ~$\frac{5}{8}$ in. This detector was positioned far enough from the target so that its acceptance angle controlled the solid angle for coincidence collection of fission-fragment pairs.

The Pb collimator and shield permitted detection of γ rays within the solid angle of 1.603×10^{-2} sr subtended by the NaI(Tl) crystal at the target center. Its saw-tooth design prevented any inner surface from being seen by both the target and the crystal; additional shielding of similar design protected against scattering from surfaces adjacent to the exit window of the vacuum chamber. A soft-iron shield for the 58-AVP photomultiplier tube also anchored the crystal and tube assembly securely in place.

Data Collection

It was necessary to carry out two separate experiments: one of four parameters (correlated energies of fission-fragment pairs and γ rays, and the time between fragment and γ-ray pulses) and

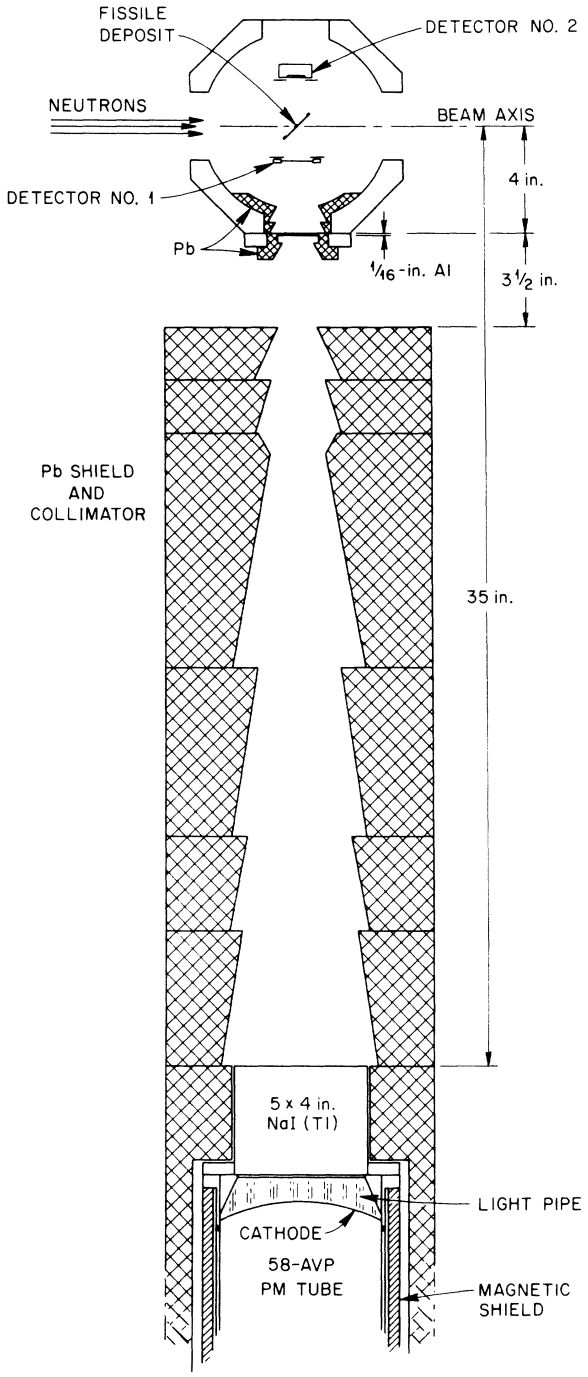

FIG. 1. Scale drawing of the experimental arrangements. The γ rays were attenuated only by the silicon wafer of detector No. 1, the thin Al window on the vacuum chamber, and the Al cover on the NaI(Tl) crystal. Scattering of the γ rays into the crystal was minimized by the interior design of the Pb collimator.

the other of two parameters (correlated fragment energies only).

Conventional circuitry was used to obtain a fast coincidence ($2\tau \sim 40$ nsec) between the fission-fragment pulses. For the four-parameter experiment a subsequent threefold coincidence requirement was imposed on pulses from (1) the fast, binary-coincidence unit; (2) a γ-ray pulseheight discriminator; and (3) a time-to-pulse-height converter, which was started by a crossover signal from detector No. 2 and stopped by a signal from the anode of the 58-AVP tube. Input pulse widths and relative timings were adjusted to provide a coincidence-collection time from ~225 nsec before fission to ~375 nsec after fission. The slow-coincidence pulse enabled linear gates on the energy and time pulses presented to a four-parameter analyzer. However, for the binary-coincidence experiment, the fast-coincidence unit controlled the linear gates and the analyzer was operated in a two-parameter mode, for the fragment pulses only.

In order to obtain the fastest possible timing from the NaI(Tl) spectrometer a double decision was made on the leading edge of the anode pulse, using constant-fraction discriminators; a fast overlap coincidence between pulses from the two levels provided the timing signal. Examples of the resolution achieved by this system can be seen in the right-hand portion of Fig. 2, which shows data taken with a ^{22}Na source using a signal from a fast plastic scintillator (1×1-in. Naton 136) to start a time-to-pulse-height converter (TPHC) and our NaI(Tl) spectrometer to stop it.

Scalers recorded the numbers of twofold and fourfold coincidences during each run for use in normalizing the γ-dependent data to the binary fission rate; γ-ray and TPHC pulses were also scaled, in order to monitor operational stability. Typical counting rates were about 255/sec and 45/sec, respectively, for detectors Nos. 1 and 2, and about 3400/sec for the γ-ray spectrometer. The coincidence rates were about 45/sec for the binary data and 0.55/sec for the four-parameter data.

The correlated data were punched event by event on paper tape; the two fragment pulse heights were recorded in 256-channel resolution and the γ-ray and time pulse heights in 1024-channel resolution. Gains of 10.4 keV/channel and 0.81 nsec/channel were used for the γ-ray and time information, respectively.

The binary-coincidence runs were interspersed among the four-parameter runs in order to ensure that both experiments properly sampled any changes in the resolution of the fragment detectors. A total of ~590 000 events were accumulated in the four-parameter runs, of which ~306 000 were later

processed as "prompt" and ~30 000 as prefission, random background events. In the binary experiment ~852 000 coincidences were recorded and processed.

An auxiliary set of four-parameter runs was also made in order to determine a correction, if necessary, for the presence of pulses from short-lived γ rays emitted from fragments already at rest on a detector. For this experiment the target was moved 1.25 in. upstream in the neutron beam, and the detector assembly was rotated rigidly about the target center, so that the target was not viewed directly by the crystal, yet the far detector remained on the axis of the Pb collimator, with a negligible shift in its distance from the crystal. Scattering and leakage effects in the "upstream" experiment were measured with independent sources, placed alternately at the two target positions. This set of experiments enables us to place an upper limit of 1.3% on the fraction of prompt γ rays in the primary experiment that originated from fragments stopped in the detectors.

Calibrations

Pulse-height calibrations for all parameters were made at the beginning and end of each run. The individual four-parameter runs were generally 7 to 8 h long; the binary runs lasted ~25 min.

The two lines from a ^{22}Na source, which was placed at the entrance to the Pb collimator, were used to check the energy response of the γ-ray spectrometer. To ensure maximum gain stability in the γ-ray spectrometer, precautions were taken throughout the experiment to maintain a constant γ-ray flux on the NaI(Tl) crystal; most importantly, these included the use of external γ-ray sources when runs were not in progress. Our efforts were rewarded by the gain remaining constant within ~10 keV for the 0.511-MeV peak and $\lesssim$12.5 keV for the 1.275-MeV peak in a total of 41 runs.

The γ-ray pulse-height spectrum was recorded in the equivalent energy range of ~85 keV to ~10 MeV. Linearity of response was verified over a wide range of γ-ray energies (0.122–6.13 MeV) with independent sources. Somewhat crude observations on capture γ rays from Al, Pb, and Ni indicated continued linearity up to 9 MeV.

The fission-fragment detectors were operated in the saturation region of pulse height versus voltage, and constant voltages were maintained across them by adjusting the applied voltages to compensate for increases in current arising from radiation damage. The fragment pulse-height spectrum parameters[16] remained acceptable throughout

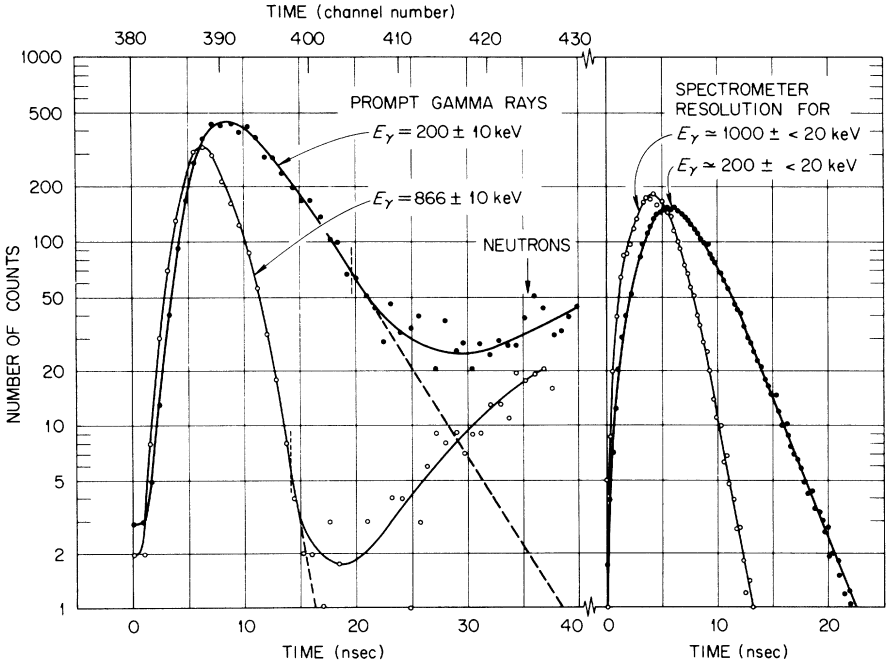

FIG. 2. Slice plots in the time versus γ-ray pulse-height distribution for the equivalent energies $E_\gamma = 200$ and 866 keV and time resolution functions measured for $E_\gamma = \sim 200$ and ~1000 keV. The distributions expected in the absence of neutrons are indicated by the dashed-line approximations to the resolution function. The vertical "ticks" on the curves show the time-channel limits used in processing the data.

the experiment. Pulser calibrations, which bracketed the spectra, checked within $\pm\frac{1}{2}$ channel (±0.22 MeV) for all runs.

The gain of the time spectrum was measured with a calibrated delay line of 259.1 ± 0.2 nsec. Pulse-height stability was checked with a pulser and two fixed-length delay lines. Drifts of up to ~5 nsec were experienced, but adjustments were made for them in processing the data.

DATA PROCESSING AND ANALYSIS

Energy calibrations for the fission-fragment detectors were obtained from the data of the binary coincidence experiment, using the formulas given by Schmitt *et al.*[17] for the pulse-height response of silicon surface-barrier detectors in the thermal-neutron-induced fission of ^{235}U. During the course of the experiment, radiation damage to the detectors produced a gradual change in their apparent gain; therefore, the runs were divided into several groups, each of which was processed with its own set of constants.

We have recently revised our computer program for processing fragment energy-correlation experiments so that pre-neutron-emission masses and kinetic energies of the fragments are calculated event by event.[18] Neutron-emission properties of the fragments are required as input, and in this experiment we have used the smoothed version of the $\bar{\nu}(m^*)$ function of Apalin *et al.*[19] that was used in the earlier work of Schmitt, Neiler, and Walter[20]; we have assumed $\bar{\nu}(m^*, E_K^*)$ to be independent of E_K^*.

Binary Experiment

In the binary experiment we obtained the mass distribution $N(m_1^*)$, the average total kinetic energy as a function of fragment mass $E_K^*(m_1^*)$ and the mass-versus-energy array $N(m_1^*, E_K^*)$, in units of 3 MeV × 3 amu, centered about mass 118. No corrections were made for dispersion effects or detector resolution and no smoothing process was used to reduce the scatter in the data. The results from this experiment agree well with the early ones of Schmitt, Neiler, and Walter.[20]

Four-Parameter Experiment

Data Sorting

The first step in processing the fourfold coincidence data was to correct for drifts in the time information. The data were inspected in records of 256 events and the channel number of the major time peak (for prompt-γ events) was determined for each record; this was then set to a "standard" channel number and the time identification x_4 of each event in the record was adjusted accordingly. A few records, in which the time peak was unduly broad or the shift in peak position was excessive, were rejected. That the time standardization was worthwhile can be seen in Fig. 3, which shows the time spectrum before and after the adjustment.

In the next stage of processing, the four correlated channel numbers were checked against their acceptable limits. For each event that satisfied the fragment and γ-ray pulse-height criteria, the γ-ray energy corresponding to the observed pulse

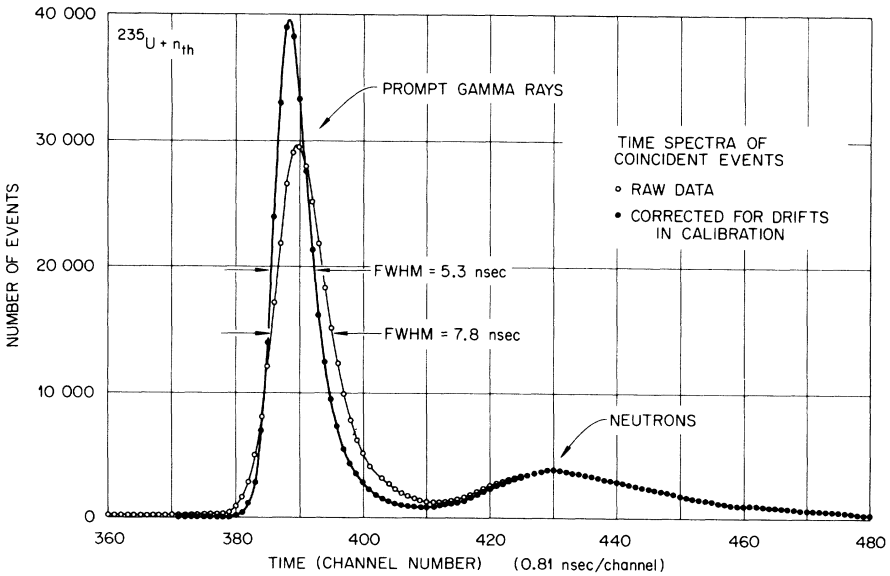

FIG. 3. Time spectra of coincident events summed over all runs, without correction for random coincidences.

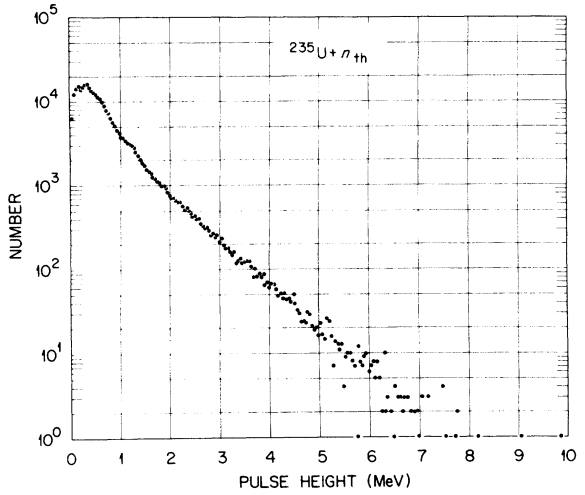

FIG. 4. Pulse-height distribution of prompt γ rays, corrected for background.

height x_3 was calculated from the ^{22}Na calibrations. If the time channel was also found to be in either of two windows, one for random, background events or one for the "prompt" events, then the fragment energies and masses were calculated for that event; otherwise, the event was omitted from further processing.

Timing Considerations

Limits were easily established for the background window Δt_r, which spanned ~225 nsec in the prefission portion of the time spectrum. Determination of the channel limits for prompt events, however, was rather onerous, because the time resolution of the NaI(Tl) spectrometer was energy-dependent. In particular, for small γ-ray pulse heights, we were unable to achieve total separation of all prompt-γ-ray and fission-neutron events. This was not unexpected, since most of the neutrons observed were emitted at ~0° with respect to the fragment's direction of motion in the laboratory system, and so traveled to the NaI(Tl) crystal with enhanced velocities. Auxiliary measurements of the time resolution function of the γ-ray spectrometer enabled us to correct for the overlap in γ-ray and neutron pulse-height distributions.

To determine this correction, the data were initially processed with a time window that was arbitrarily wide compared with the time peak. All

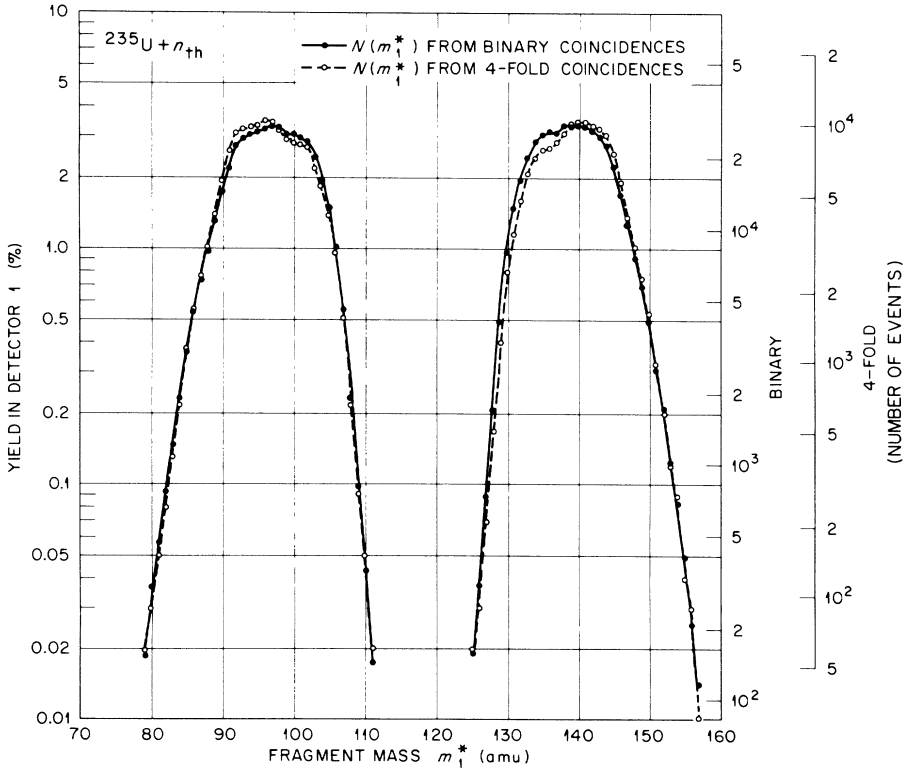

FIG. 5. Mass distributions. The solid curve is the result derived from the binary experiment. The dashed curve, with open circles, is obtained from the γ-dependent experiment by processing the events contained in the prompt time-window with uniform weights, $g = 1$.

acceptable events were summed over all masses, with background corrections included, and assembled in a pulse-height array of x_3 vs x_4. Slice plots were made for constant values of x_3 in steps suited to the rate of change in the peak widths, which varied from a maximum of ~12.3 nsec (full width at half maximum) for $E_\gamma = 100$ keV down to a constant value of ~4.4 nsec for $E_\gamma \geq 850$ keV. Figure 2 shows two of these slice plots and two measurements of the resolution function. There is general agreement in the energy dependence of the peak widths and shifts in position for the two sets of measurements.

Figure 2 also shows that the resolution function falls off with a constant slope on a semilog plot. Therefore, for each slice plot we approximated the resolution function by fitting straight lines to the trailing edges of the prompt time peaks and determined an upper channel limit for time which excluded neutron-associated events. The prompt time window $\Delta t_p(E_\gamma)$ was then constructed as a function of γ-ray energy using a fixed lower limit and matching the upper limit to these cutoff channels. A correction factor was also obtained as a function of E_γ; it was equal to the ratio of the total area under the approximated resolution function to the area selected by this window.

Slice plots were also made from arrays of x_3 vs x_4 in which the data were summed over limited mass ranges. These showed that the net broadening of the prompt time peak from mass-dependent effects ranged from ~0.8 nsec (full width at half maximum) for $E_\gamma = 0.2$ MeV down to 0.2 nsec for $E_\gamma \geq 1.0$ MeV.

The pulse-height distribution of the γ rays included in the prompt time window, corrected only for the background of random events, is shown in Fig. 4.

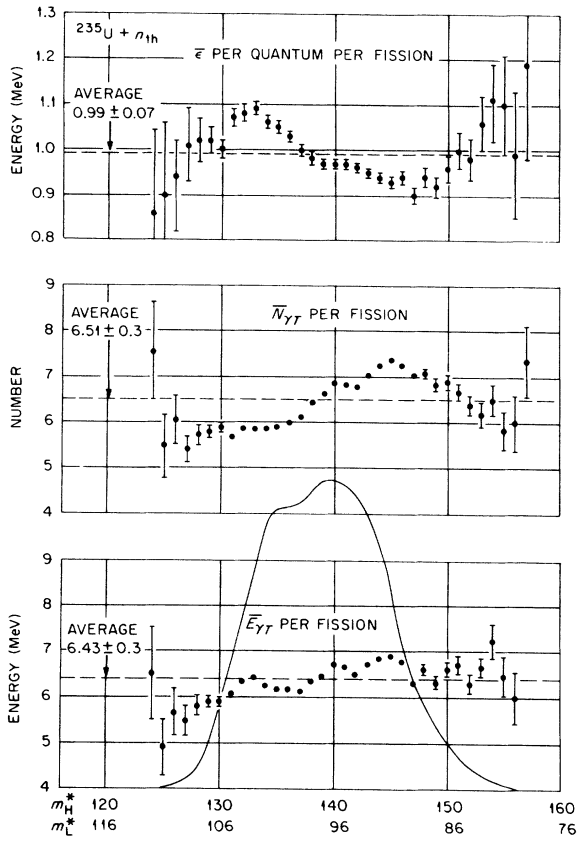

FIG. 6. The average total energy $\bar{E}_{\gamma T}$ and average total number $\bar{N}_{\gamma T}$ of γ rays emitted per fission as functions of complementary mass pairs. The top part of the figure shows the average photon energy $\bar{\epsilon} = \bar{E}_{\gamma T}/\bar{N}_{\gamma T}$. Error bars, including statistical uncertainties, are shown except where they are commensurate with the size of the points. These functions are averaged over the binary mass distribution to obtain the values given for the average total yields $\langle \bar{E}_{\gamma T} \rangle$, $\langle \bar{N}_{\gamma T} \rangle$, and $\langle \bar{\epsilon} \rangle$ per fission.

γ-Weighted Mass Distributions

As indicated above, each event in the four-parameter experiment is tagged as "random" or "prompt" or is rejected. A pre-neutron-emission mass distribution, corrected for background, is accumulated by adding 1 for each prompt event and subtracting $R(E_\gamma)$ for each random event, where $R(E_\gamma) = \Delta t_p(E_\gamma)/\Delta t_r$. The distribution thus obtained is compared with the distribution from the binary experiment in Fig. 5. Although they are nearly the same, it is evident that the differences between them vary in magnitude and direction as a function of fragment mass.

The mass distributions required for determining the average number or average energy of the γ rays, labeled $N_N(m_1^*)$ and $N_E(m_1^*)$, respectively, are obtained through use of weighting factors g_N or g_E, which are functions of E_γ. (See Appendix

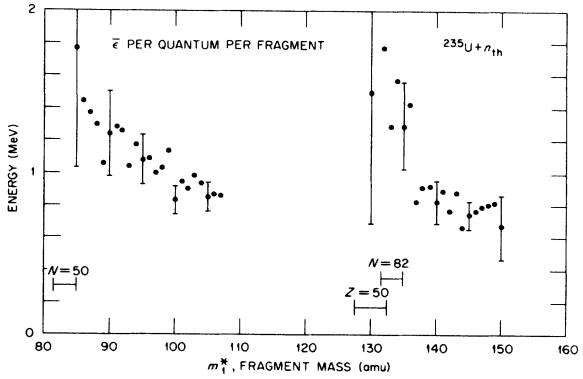

FIG. 7. Average photon energy $\bar{\epsilon}$ per fragment. Sample error bars are shown at 5-amu intervals.

II.) A similar procedure is followed, but g_n or g_E (instead of 1) is added for each prompt event, and $R(E_\gamma)g_N$ or $R(E_\gamma)g_E$ is subtracted for each background event. The corresponding mass-versus-energy arrays $N_N(m_1^*, E_K^*)$ and $N_E(m_1^*, E_K^*)$ are constructed at the same time.

Determination of $\bar{N}_\gamma$ and $\bar{E}_\gamma$

The results for the average number and average energy of the γ rays are obtained from Eqs. (8) and (9). The quantities contained therein are evaluated as follows:

(a) n_M is the total number of binary fissions in which mass M goes to detector No. 1 during the four-parameter experiment. It is calculated by multiplying the fractional yield at mass $m_1^* = M$ in the binary mass distribution by the number S_2 of the twofold coincidences scaled during the four-parameter runs; this product is corrected for dead-time loss in the paper-tape punch, by the ratio of the number of fourfold events punched P_4 to the number scaled S_4. Thus,

$$n_M = [N(M)/N(m_1^*)]_{\text{binary}}\, S_2(P_4/S_4). \tag{12}$$

(b) $\beta_M = v/c$ is calculated from the mass M and the average $E_K^*(m_1^*)$ from the binary experiment.

(c) $N(M) = n_{\gamma M}/p_\gamma$ is the entry at mass M in the γ-weighted distribution $N_N(m_1^*)$ or $N_E(m_1^*)$.

We draw on the fact that the four-parameter and binary experiments were carried out under identical experimental arrangements and instrumentation and that masses and energies were derived from the two sets of data by exactly the same method; thus, the mass distributions from both experiments should reflect the same effects of dispersion and resolution. Consequently, we use values for n_M/n_{A-M} that are taken directly from the mass distribution derived from the binary experiment. Since neither mass distribution is smoothed in any way, this procedure will permit inherent statistical scattering of the data to introduce some fluctuations in the final results for the average number $\bar{N}_\gamma$ and the average energy $\bar{E}_\gamma$ of the γ rays

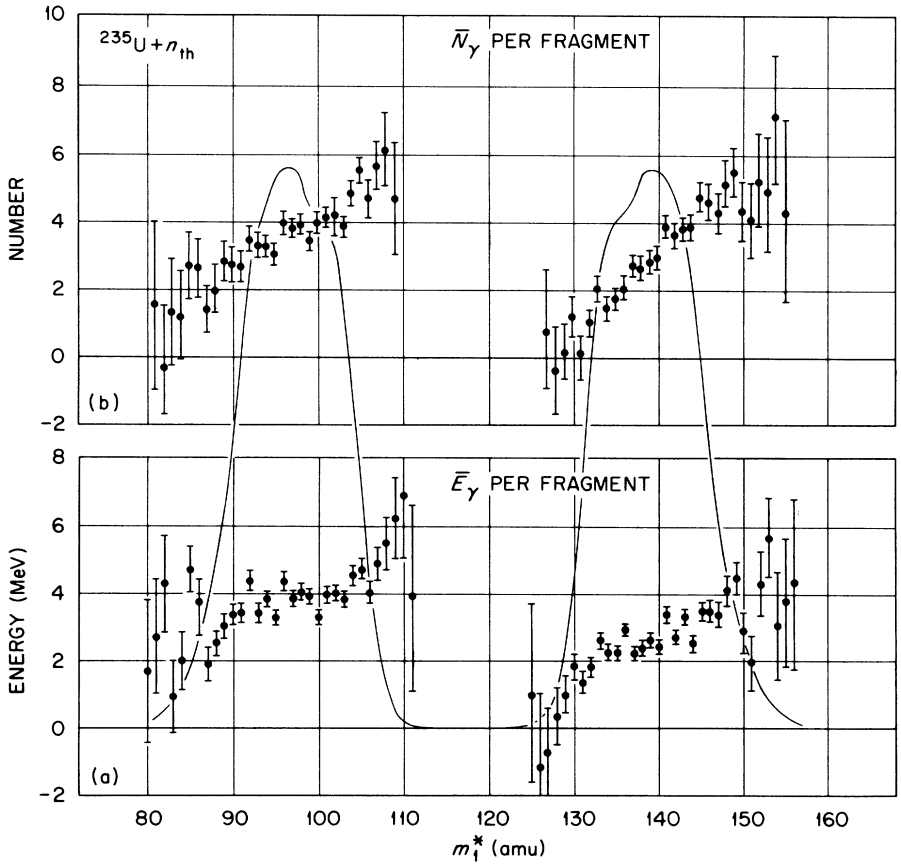

FIG. 8. (a) The average energy $\bar{E}_\gamma$ and (b) average number $\bar{N}_\gamma$ of γ rays emitted as functions of fragment mass. The binary mass yield is sketched in for reference.

emitted as a function or fragment mass [Eq. (8)] and as a function of complementary fragment pairs [Eq. (9)].

Equations (8) and (9) are used to obtain these same quantities as functions of fragment mass and energy in the arrays $\bar{N}_\gamma(E_K^*, m_1^*)$ and $\bar{E}_\gamma(E_K^*, m_1^*)$. Here, however, the β's were calculated for the mass and energy assigned to the center of each interval in the two-dimensional arrays.

Because of the spread in the velocities of the fission fragments and the different distances to the detectors, these results may contain a few events (up to 1.3%) in which the fragment was at rest, before the γ ray was emitted. No correction has been made for these events, since the results for $\bar{N}_\gamma$ and $\bar{E}_\gamma$ for single fragments would be altered only slightly and those for both fragments $\bar{N}_{\gamma T}$ and $\bar{E}_{\gamma T}$ are independent of these events.

RESULTS AND DISCUSSION

The experimental results are presented in terms of pre-neutron-emission quantities. In Figs. 6–10 they are given as functions of fragment mass and in Figs. 11–13 as functions of total fragment kinetic energy. Absolute values for the average number and average energy are given; the error bars include only the statistical uncertainties, whereas the values quoted for the over-all averages in Fig. 6 include both statistical uncertainties and our estimates of systematic uncertainties, excluding anisotropy. We have assumed in our analysis that the γ rays are emitted isotropically in the fragment center-of-mass systems; deviations from isotropy give rise to a correction factor which is the ratio of the average total yield to the yield at 0° (or 180°). If the anisotropy determination of Armbruster, Labus, and Reichelt[13] is used, our results for both energy and number of γ rays emitted would be decreased by ~6%.

The most significant sources of systematic uncertainties are related to possible inaccuracies in evaluating the weighting factors g_N and g_E and the correction factor for the energy-dependent time-window cutoff. It was found, in early phases

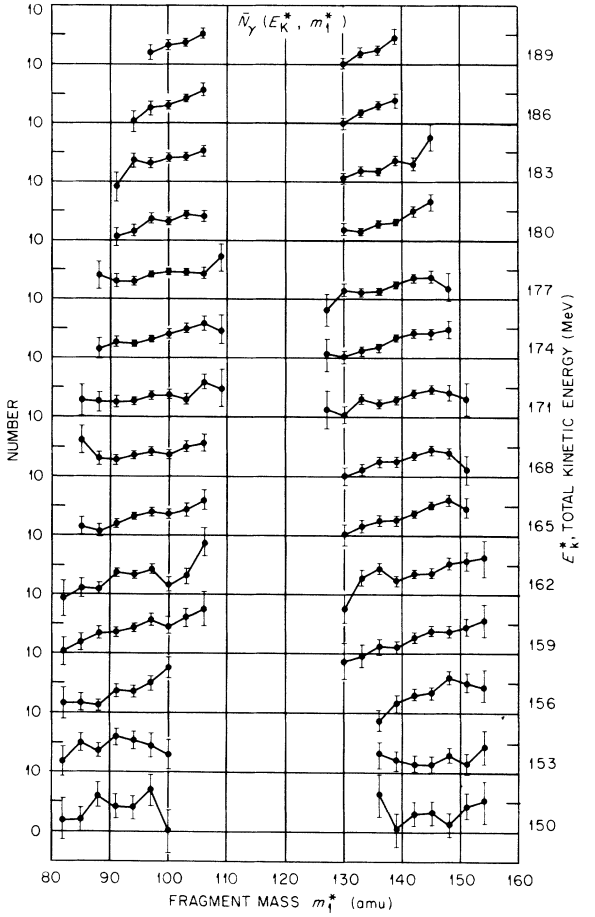

FIG. 9. Slice plots at constant kinetic energy E_K^* in the 3-MeV × 3-amu array $\bar{N}_\gamma(E_K^*, m_1^*)$.

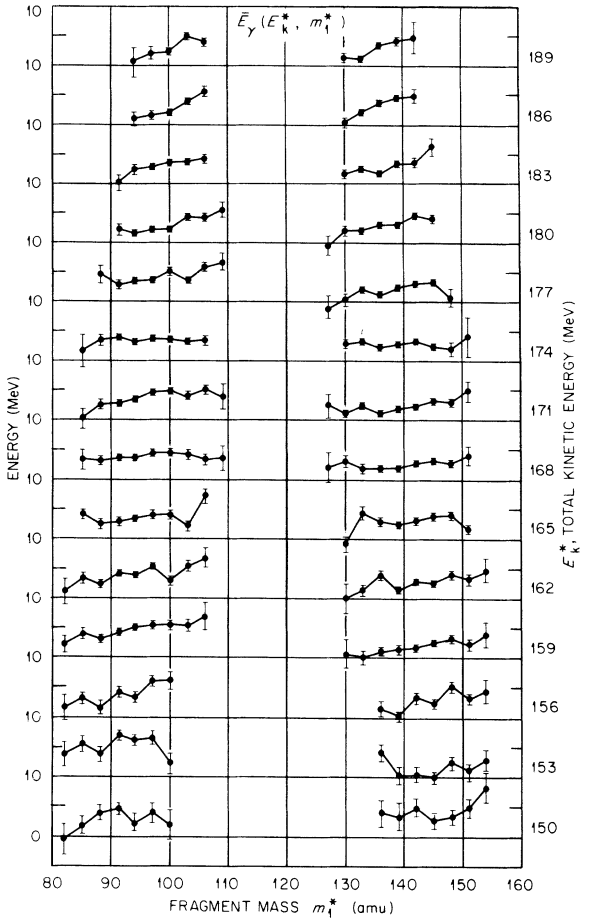

FIG. 10. Slice plots at constant kinetic energy E_K^* in the 3-MeV × 3-amu array $\bar{E}_\gamma(E_K^*, m_1^*)$.

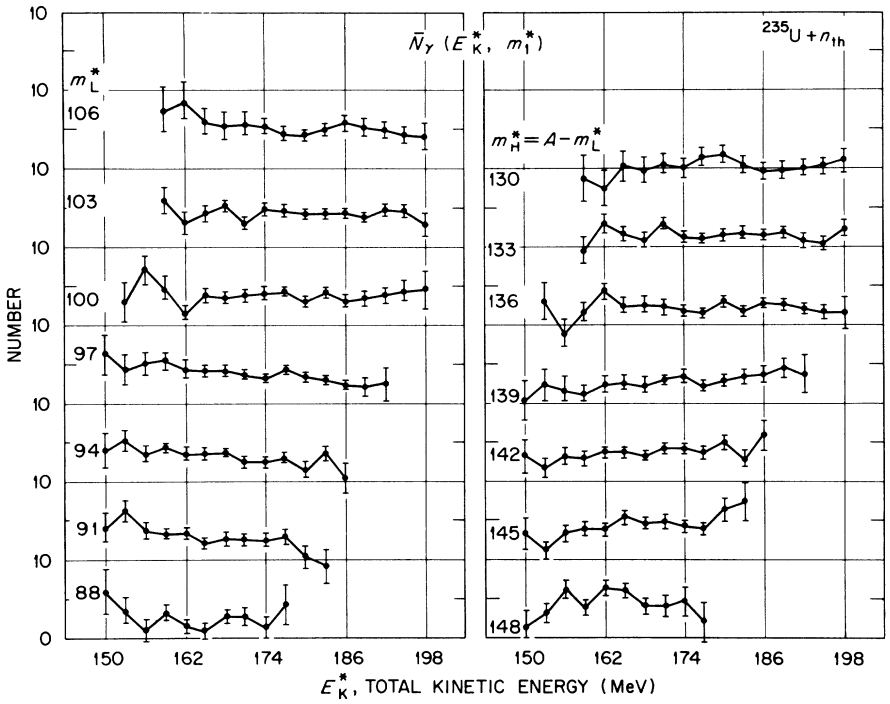

FIG. 11. Slice plots at constant mass m_1^* in the 3-MeV × 3-amu array $\bar{N}_\gamma (E_K^*, m_1^*)$.

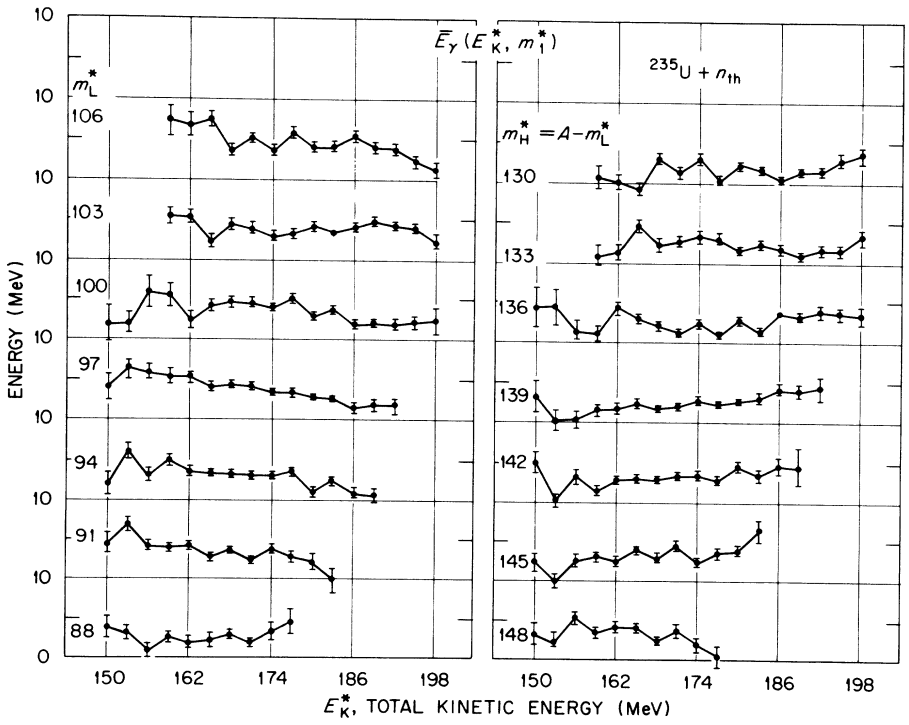

FIG. 12. Slice plots at constant mass m_1^* in the 3-MeV × 3-amu array $\bar{E}_\gamma (E_K^*, m_1^*)$.

of the work, that the method used for obtaining the weighted averages (Appendix II) eliminates any strong dependence of the g's on the exact formulation of the response matrix. The intrinsic efficiency of the detector ϵ_T and the solid angle Ω of detection can be calculated quite accurately, leaving the transmission function α as the factor most susceptible to errors of evaluation. However, as seen in Appendix II, measurements with the calibrated sources enabled us to correct calculated values of α for additional scattering effects of materials in the vicinity of the detector. The ±5% uncertainties applied to the over-all averages of $\bar{N}_{\gamma T}$, $\bar{E}_{\gamma T}$, and $\bar{\epsilon}$ should be adequate to include systematic errors from all sources.

Figure 6 shows the average total number $\bar{N}_{\gamma T}$ and the average total energy $\bar{E}_{\gamma T}$ of prompt γ rays emitted per fission as functions of complementary fragment pairs. Scales for both light- and heavy-fragment mass are shown along the abscissa. The average photon energy, or energy per quantum $\bar{\epsilon}$, is plotted in the uppermost section of the figure.

Both $\bar{N}_{\gamma T}$ and $\bar{E}_{\gamma T}$ generally increase with increasing mass asymmetry, although a peak in $\bar{N}_{\gamma T}$ occurs at $m_H^*/m_L^* \sim 145/91$. A corresponding minimum occurs in $\bar{\epsilon}$ at approximately the same mass ratio. A rather pronounced peak occurs in $\bar{\epsilon}$ at $m_H^*/m_L^* \sim 132/104$. Nuclei in the region about $m_H^* \sim 132$ have a near doubly magic character ($Z=50$, $N=82$), and therefore are stiffer than their neighbors on either side. If prompt γ rays originate with vibrational cascades, as has been suggested by Johansson and Kleinheinz,[21] it is reasonable that such a peak should occur.

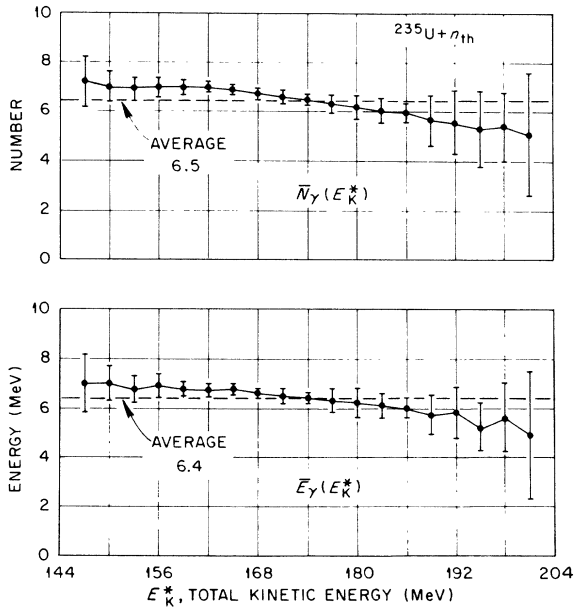

FIG. 13. The average total number and energy of γ rays emitted per fission as functions of total kinetic energy. These results are averages, over the binary mass yield, of the plots in Figs. 11 and 12. The dashed lines are averages over the kinetic energy distribution.

Moving toward greater asymmetry, into a region where both fragments are softer, we see that $\bar{\epsilon}$ decreases until $m_H^*/m_L^* \sim 150/86$. Here, the effects of the neutron magic number $N=50$ become evident: The vibrational energy increases as the light fragment becomes stiffer and $\bar{\epsilon}$ for the γ-ray cascade begins to increase again. Figure 7 shows the decrease of $\bar{\epsilon}$ as one moves away from the magic configurations in the lower-mass portions of both fragment groups.

Figure 8 shows the average number and energy of γ rays emitted from single fragments as functions of fragment mass. Average values for the light (L) and heavy (H) fragment groups are:

$$\langle \bar{N}_{\gamma L} \rangle = 3.63 \pm 0.4 ,$$

$$\langle \bar{N}_{\gamma H} \rangle = 2.88 \pm 0.3 ,$$

$$\langle \bar{E}_{\gamma L} \rangle = 3.78 \pm 0.4 \text{ MeV} ,$$

$$\langle \bar{E}_{\gamma H} \rangle = 2.66 \pm 0.3 \text{ MeV} ,$$

where the uncertainties include both statistical and estimated systematic errors other than those associated with anisotropy.

As seen in earlier relative measurements,[1, 10, 13, 22] these functions exhibit a sawtooth behavior similar to the one that characterizes the emission of neutrons as a function of fragment mass.[19] This behavior, together with the high values attained for $\langle \bar{E}_{\gamma T} \rangle$, relative to expectations based on statistical-model calculations,[23, 24] has been used as an indication that γ decay competes effectively with neutron decay in the dissipation of initial fragment excitation energy.[21, 25] Since γ decay is most important in reducing the angular momentum of the initial fragments, this observation would seem to indicate that the heavier fragments in each of the two groups are formed with higher angular momenta.

If we assume for the moment that all prompt γ rays emitted in fission and measured in this experiment ($\tau \lesssim 5$ nsec) arise from collective $E2$ transitions in the fragments after prompt neutron emission has taken place,[13, 21, 26] and if the angular momentum carried away by prompt neutron emission is small, the average spin $\bar{J}$ of a pre-neutron-emission fragment is approximately twice the average number of γ rays emitted from the fragment. On this basis the angular momenta of the fragments range from low values, 0 to $2\hbar$ for fragment nuclei containing near-magic numbers of nucleons ($m_1^* \sim 84$ with $N \sim 50$ and $m_1^* \sim 130$ with

$Z \sim 50$, $N \sim 82$), to about $10\hbar$ for deformed fragment nuclei which occur at the heavy ends of the two fragment groups. Averages for the light and heavy groups would be $\sim 7\hbar$ and $\sim 5\hbar$, respectively; the over-all average would be $\sim 6.4\hbar$, consistent with values obtained from other recent experiments.[13]

In Fig. 9 we show the average number of γ rays emitted from single fragments versus fragment mass, for 3-MeV intervals in total kinetic energy. The average energy of γ rays emitted from single fragments is plotted similarly in Fig. 10. The sawtooth behavior for both $\bar{N}_\gamma$ and $\bar{E}_\gamma$ is apparent for most of the total-kinetic-energy groups, although it is somewhat weaker for the lower E_K^* groups.

In Figs. 11 and 12 we show the average number and energy, respectively, of γ rays emitted from single fragments as functions of total fragment kinetic energy, for mass groups in 3-amu intervals. Most of the curves are rather flat, showing little, if any, dependence on total kinetic energy. The curves for masses $m_H^* = 139$ and 142, and $m_L^* = 94$ and 97, corresponding to the peaks of the mass distribution, are statistically most significant and do show certain trends: For the heavy fragment both $\bar{E}_\gamma$ and $\bar{N}_\gamma$ increase with increasing E_K^*, while for the light fragment they both decrease with increasing E_K^*. These observations may imply that the light fragment is more deformed and has higher $\bar{J}$ for the low-kinetic-energy events than for the high-kinetic-energy events; for the heavy fragment just the reverse occurs.

Figure 13 shows $\bar{E}_{\gamma T}$ and $\bar{N}_{\gamma T}$ versus E_K^*, where they are the average total γ-ray energy and number for both fragments. Both of these quantities are observed to decrease with increasing E_K^*, as might be expected since higher total kinetic energies are associated with less-deformed fragment shapes and, therefore, with lower excitation energies.

Returning to the sawtooth behavior of the single-fragment number and energy results shown in Fig. 8, we have noted the similarity of these curves with the well-known sawtooth curve for the average number of neutrons emitted as a function of fragment mass.[19] Nifenecker *et al.*[14] have studied the correlation of neutron and γ emission for ^{252}Cf spontaneous fission and have concluded that a linear relationship exists between the average total γ-ray energy emitted by a given fragment and the average number of neutrons emitted by the same fragment; they point out that this relationship may be obtained because of a linear increase of average fragment spin with excitation energy. Our results are not inconsistent with these conclusions.

Thomas and Grover[25] have discussed the competition of neutron and γ-ray emission in fission and have obtained 7.1 MeV as the average total γ-ray energy for the 140/96 mass split; this compares with our value of $\bar{E}_{\gamma T} = 6.7$ MeV. They obtain an average photon energy of 0.9 MeV, compared to our value of $\bar{\epsilon} = 0.97$ MeV for this mass split.

The over-all average total number and energy of prompt γ rays obtained from the present work are compared in Table I with results of other experiments. The table is divided into two sections which pertain to different ranges of γ-ray energy accepted in the various experiments. The entries in each section are ordered according to the time interval defined as prompt-coincidence time between fission and γ-ray detection. This tabulation shows a strong correlation between the length of the time interval and the values obtained for $\langle \bar{N}_{\gamma T} \rangle$ and $\langle \bar{E}_{\gamma T} \rangle$. The results of the present work agree well with those of Verbinski and Sund[9] but are in

TABLE I. Average numbers and energies of prompt γ rays emitted in the fission of $^{235}\mathrm{U} + n_{\mathrm{th}}$.

γ energy (MeV)	Time interval (nsec)	$\langle \bar{N}_{\gamma T} \rangle$ (γ/fission)	$\langle \bar{E}_{\gamma T} \rangle$ (MeV/fission)	$\langle \bar{\epsilon} \rangle$ (MeV/γ)	Source
			Part (a)		
0.09 – 10.0	~5	6.51 ± 0.3	6.43 ± 0.3	0.99	This work
0.14 – 10.0	~10	6.69 ± 0.3	6.51 ± 0.3	0.97	Verbinski and Sund [a]
0.14 – 10.0	≤69	7.45 ± 0.32	7.18 ± 0.26	0.96	Peelle and Maienschein [b]
0.1 – 2.5	220	7.9 ± 0.1	9.5 ± 0.2	1.20	Rau [c]
			Part (b)		
0.01 – 10.5	≤69	8.13 ± 0.35	7.25 ± 0.26	0.87	Peelle and Maienschein [b]
0.03 – 10.4	~70	8.1 ± 0.8	7.0 ± 0.7	0.90	Preliminary results [d]
0.03 – 10.4	275	8.6 ± 0.8	7.4 ± 0.7	0.86	Preliminary results [d]

[a] Reference 9.
[b] Reference 8.
[c] Reference 28.
[d] Reference 27.

disagreement with the others.

Part (b) of the table includes preliminary results of Pleasonton[27] for a wider range of γ-ray energies and broader time intervals. Those results were obtained from a similar four-parameter experiment which employed a shorter flight path (45 cm) to the NaI(Tl) crystal, included a ^{6}LiH absorber inside the γ-ray collimator, and recorded the times of coincident events in poorer resolution. It appears from the time spectrum shown in Fig. 3, that there are too few short-lived delayed γ rays emitted within 5–70 nsec after fission to account for the higher preliminary results. We therefore attribute the discrepancies between the two sets of results to the leakage of neutrons through the ^{6}LiH absorber and the consequent analysis of an inseparable admixture of neutron and γ-ray events in the previous experiment.

The fact that the preliminary results of Pleasonton[27] are in closer agreement with those of Peelle and Maienschein[8] and of Rau[28] suggests that their experiments may also have included detection of some neutrons, in spite of the precautions taken to exclude them.

Only a qualitative comparison can be made between the present results and the early work of Maier-Leibnitz, Schmitt, and Armbruster[1] because their results are presented on a relative scale. Similar trends are seen in all comparable figures: the sawtooth shapes of $\bar{N}_\gamma$ and $\bar{E}_\gamma$, including the leveling off of $\bar{E}_\gamma$ in the regions of the peaks in the mass distribution; the maxima and minima in $\bar{E}_{\gamma T}$ and $\bar{\epsilon}$ in the regions of $m_H/m_L = 145/91$ and $132/104$; and the decreases of $\bar{\epsilon}(m)$ in the higher mass portions of both fragment groups.

In conclusion, it has been our principal purpose in this paper to describe the experiment and its analysis, and to present detailed experimental results for thermal-neutron fission of ^{235}U. A series of experiments on other thermal-neutron fission reactions is in progress in an effort to obtain further systematic information on prompt γ decay of fission fragments. A more comprehensive analysis of all the data will be discussed along with those results.

ACKNOWLEDGMENTS

The authors would like to express their appreciation to H. Maier-Leibnitz, who proposed the original experiment from which this work developed, and to P. Armbruster, who collaborated in the early work, for helpful discussions and for their continued interest.

We are grateful to N. W. Hill, for his valuable advice and assistance in developing the fast timing circuitry for our γ-ray spectrometer, and to V. V. Verbinski and G. T. Chapman for helpful discussions. We wish to thank E. H. Kobisk, H. Hunter, and associates for the preparation of the ^{235}U target and the operating staff of the Oak Ridge research reactor for their contributions to the smooth conduct of the experiment.

APPENDIX I. RESPONSE MATRIX

A response matrix was developed which combines information from measured pulse-height distributions with Monte Carlo calculations[29] of response functions for monoenergetic γ-ray sources in the geometry of the experiment.

Calibrated sources,[30] ranging in energy from 0.122 to 1.836 MeV, whose absolute intensities were known to an accuracy of ~1%, were placed in the position normally occupied by the fissile target. The measured pulse-height distributions were stripped and values obtained for peak-to-total ratios f_m and for the full width at half maximum amplitude ΔE (MeV). Assuming the photopeaks to be Gaussian in shape, their standard deviations were found from the relationship $\sigma = \Delta E/2.3548$. From a plot of σ vs ΔE, at the calibration energies, we derived the resolution function for our spectrometer:

$$\sigma = 0.0314E^{1/2} + 0.016\,11E + 0.008\,45 . \qquad \text{(A1)}$$

This function was used in the Monte Carlo program MORN (originated by Zerby and Moran[29] and revised by Rodda[31]) to calculate pulse-height distributions, photofractions f_c, and total counter intrinsic efficiencies ϵ_T for each calibration line. Good fits to the experimental data were obtained for peak shapes and a very satisfactory comparison was found for the photo- and single-escape peaks of the 6.13-MeV line of ^{16}N. However, the calculations gave lower Compton distributions and higher peak-to-valley ratios than those in the measured distributions; such differences were expected, since the program neglects the effects of scattering in materials in the vicinity of the detector.

These discrepancies do not affect our results, since no attempt was made, in our response matrix, to describe the fine details of the pulse-height distributions. They were approximated by assuming that the entire photopeak is contained in a single energy interval and the Compton distribution is distributed uniformly from the minimum energy bias to the energy of the photoline, i.e., the center of the photopeak. (See, for example, Bienlein and Pleasonton[32] for the propriety of this procedure.)

Values of the photofractions to be used in generating the response matrix were determined from the results of the MORN program, with the calcu-

TABLE II. Response matrix.

Pulse height (MeV)	Energy (MeV) $i \backslash j$	0.150 1	0.294 2	0.478 3	0.705 4	0.979 5	1.30 6	1.69 7	2.13 8	2.65 9	3.24 10	3.92 11	4.69 12	5.57 13	6.56 14	7.68 15	8.94 16
0.150	1	1.000	0.105	0.092	0.080	0.068	0.057	0.047	0.039	0.032	0.026	0.022	0.019	0.016	0.014	0.012	0.011
0.294	2	0.0	0.895	0.121	0.106	0.089	0.075	0.062	0.051	0.042	0.034	0.029	0.024	0.021	0.018	0.016	0.014
0.478	3	0.0	0.0	0.786	0.132	0.112	0.093	0.077	0.064	0.052	0.043	0.036	0.031	0.026	0.023	0.020	0.017
0.705	4	0.0	0.0	0.0	0.682	0.136	0.116	0.101	0.078	0.064	0.053	0.044	0.037	0.032	0.028	0.024	0.021
0.979	5	0.0	0.0	0.0	0.0	0.595	0.137	0.122	0.096	0.076	0.063	0.053	0.045	0.038	0.033	0.029	0.025
1.30	6	0.0	0.0	0.0	0.0	0.0	0.523	0.133	0.127	0.091	0.074	0.062	0.053	0.045	0.039	0.034	0.030
1.69	7	0.0	0.0	0.0	0.0	0.0	0.0	0.458	0.140	0.116	0.087	0.072	0.062	0.053	0.046	0.040	0.035
2.13	8	0.0	0.0	0.0	0.0	0.0	0.0	0.0	0.406	0.168	0.114	0.084	0.072	0.062	0.053	0.046	0.041
2.65	9	0.0	0.0	0.0	0.0	0.0	0.0	0.0	0.0	0.359	0.177	0.108	0.083	0.071	0.061	0.053	0.047
3.24	10	0.0	0.0	0.0	0.0	0.0	0.0	0.0	0.0	0.0	0.329	0.181	0.102	0.081	0.070	0.061	0.054
3.92	11	0.0	0.0	0.0	0.0	0.0	0.0	0.0	0.0	0.0	0.0	0.309	0.182	0.097	0.080	0.070	0.061
4.69	12	0.0	0.0	0.0	0.0	0.0	0.0	0.0	0.0	0.0	0.0	0.0	0.291	0.180	0.093	0.079	0.070
5.57	13	0.0	0.0	0.0	0.0	0.0	0.0	0.0	0.0	0.0	0.0	0.0	0.0	0.277	0.179	0.090	0.079
6.56	14	0.0	0.0	0.0	0.0	0.0	0.0	0.0	0.0	0.0	0.0	0.0	0.0	0.0	0.262	0.171	0.089
7.68	15	0.0	0.0	0.0	0.0	0.0	0.0	0.0	0.0	0.0	0.0	0.0	0.0	0.0	0.0	0.254	0.160
8.94	16	0.0	0.0	0.0	0.0	0.0	0.0	0.0	0.0	0.0	0.0	0.0	0.0	0.0	0.0	0.0	0.245
ΔE_j(MeV)		0.124	0.163	0.205	0.249	0.299	0.353	0.413	0.479	0.553	0.633	0.723	0.822	0.931	1.05	1.18	1.33
ϵ_T		0.990	0.970	0.917	0.872	0.826	0.780	0.744	0.716	0.693	0.677	0.668	0.665	0.664	0.665	0.670	0.678

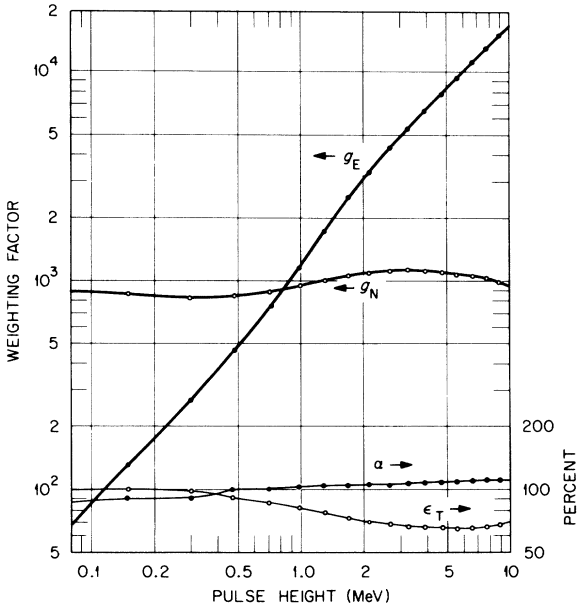

FIG. 14. Weighting factors g_N and g_E derived from the response matrix of Table II. The total intrinsic efficiency of the NaI(Tl) crystal and the effective transmission factor α are plotted against the scale on the right. The curves in this figure are applicable only to the specific physical arrangements of this experiment.

lated photofraction corrected by a factor f_m/f_c obtained from the comparison between the measured and calculated pulse-height distributions at known energies.

The pulse-height response for a monoenergetic γ ray of energy E_j is constructed in a column of elements w_{ij}, where the index i specifies the measured pulse heights. Following the earlier assumption of a Gaussian shape for the photopeak, and noting that more than 99% of such a distribution lies in an interval of ± 2.7 units of σ about its mean, we chose the width of each column to be $\Delta E_j = 5.4\sigma(E_j)$, where σ is calculated by Eq. (A1). The diagonal element w_{jj} contains the entire photofraction, plus a portion of the Compton distribution. The remainder of the Compton distribution is divided among elements with $i<j$ in proportion to their widths $\Delta E_i/E_j$. Escape peaks are assumed to have Gaussian distributions and thus their contributions are also spread over energy ranges of 5.4σ, where σ is calculated for each escape-peak energy; their contents are then added proportionally to those elements w_{ij} $(i \leq j)$ that overlap their energy ranges. Each column of the matrix is normalized to a total response of unity.

Table II gives the complete triangular matrix, with identification of the energies E_j from which

it was constructed and the widths of the columns ΔE_j associated with them. Values of the total intrinsic efficiency ϵ_T, as calculated by program MORN, are also tabulated for each E_j.

APPENDIX II. METHOD FOR OBTAINING A WEIGHTED AVERAGE OVER A SPECTRUM (SEE REF. 15)

If a source emits $N(E_0)$ γ rays of energy E_0 they are observed in a scintillation spectrometer as a continuous pulse-height distribution which extends from the full energy of the photopeak down to zero, i.e.,

$$N(x, E_0) = N(E_0)\, p(E_0) w(x, E_0)\,, \tag{A2}$$

where $p(E_0)$ is the probability for detection and $w(x, E_0)$ describes the pulse-height response for a γ ray of energy E_0.

If a continuous spectrum of γ rays is emitted, such that $N(E)dE$ is the number emitted in an interval dE, then the total number is given by

$$N = \int_0^{E_{\max}} N(E)dE \tag{A3}$$

and the observed pulse-height distribution becomes

$$N(x) = \int_0^{E_{\max}} N(E)\, p(E) w(x, E)dE\,. \tag{A4}$$

It is desired to find a weighting function $g(x)$ to relate the total number of γ rays from the source, directly to the distribution:

$$N = \int_0^{x = E_{\max}} N(x) g(x)dx\,. \tag{A5}$$

Substituting the expression for $N(x)$ from Eq. (A4) into Eq. (A5) we have

$$N = \int_0^{E_{\max}} \int_0^{x = E_{\max}} N(E)\, p(E) w(x, E) g(x)dx dE\,. \tag{A6}$$

Comparison of Eq. (A6) with Eq. (A3) gives us the relation

$$p(E) \int_0^{E_{\max}} w(x, E) g(x)dx = 1\,, \tag{A7}$$

which determines the weighting function $g(x)$. This function can be obtained by solving a system of linear equations for discrete values $g_i(x)$ and passing a smooth curve through a plot of their values. The response function $w(x, E)$ for our spectrometer is the matrix developed in Appendix I, for 16 values of pulse height x_i and γ-ray energy E_j.

In order to obtain the probabilities of detection $p_j = p(E_j)$ we again made use of the measurements with the calibrated sources. The counting rates expected in the absence of absorption or scattering were calculated for each source from the equation

$$N_c = N_0 \Omega \epsilon_T \tag{A8}$$

using the known intensities of the sources for N_0, $\Omega = 1.603 \times 10^{-2}$ sr (calculated from the geometry of the experiment), and the values obtained from program MORN for ϵ_T (see Appendix I). The ratio of the measured counting rates N_m (above an energy bias of 0.09 MeV) to those calculated N_c defined the effective transmission function α_m of the spectrometer. Transmission factors α_c were calculated for the known amounts of absorbing materials (see Fig. 1) and compared with the effective values α_m. By fitting a smooth curve through a plot of α_m/α_c vs $\ln E$ a function was obtained for correcting values of α_c at the energies E_j specified in the response matrix, to give $\alpha(E_j)$. The quantity p_j is then calculated from the expression

$$p_j = \Omega \alpha(E_j) \epsilon_T(E_j)\,. \tag{A9}$$

The g_i may now be obtained, as indicated above, by sequentially solving a system of linear equations based on Eq. (A7), as follows:

$$\begin{aligned} 1/p_1 &= g_1 w_{11} \\ 1/p_2 &= g_1 w_{12} + g_2 w_{22} \\ &\vdots \\ 1/p_j &= g_1 w_{1j} + g_2 w_{2j} + g_3 w_{3j} + \cdots + g_j w_{jj}\,. \end{aligned} \tag{A10}$$

At each step, all quantities are known except the new g_i.

To determine the average total energy emitted by the source, a parallel analysis is followed, beginning with the relation

$$E = \int_0^{E_{\max}} EN(E)dE \tag{A11}$$

and ending with a system of equations:

$$E_j/p_j = g_1' w_{1j} + g_2' w_{2j} + g_3' w_{3j} + \cdots + g_j' w_{jj}\,. \tag{A12}$$

The weighting factors g_N for average number of γ rays, and g_E for average γ energy, are plotted in Fig. 14. The functions $\alpha(E_j)$ and $\epsilon_T(E_j)$ are also shown.

†Research sponsored by the U. S. Atomic Energy Commission under contract with Union Carbide Corporation.

[1]H. Maier-Leibnitz, H. W. Schmitt, and P. Armbruster, in *Proceedings of the Symposium on the Physics and Chemistry of Fission, Salzburg, 1965* (International Atomic Energy Agency, Vienna, Austria, 1965), Vol. II, p. 143.

[2]W. John, J. J. Wesolowski, and F. Guy, Phys. Letters 30B, 340 (1969).

[3]E. Cheifetz, R. C. Jared, S. G. Thompson, and J. B. Wilhelmy, Phys. Rev. Letters 25, 38 (1970).

[4]J. B. Wilhelmy, S. G. Thompson, R. C. Jared, and E. Cheifetz, Phys. Rev. Letters 25, 1122 (1970).

[5]J. B. Wilhelmy, E. Cheifetz, R. C. Jared, S. G. Thompson, H. R. Bowman, and J. O. Rasmussen, Lawrence Berkeley Laboratory Report No. LBL-256, 1971 (unpublished).

[6]F. Horsch, to be published.

[7]F. Horsch, Institut für Angewandte Kernphysik, Karlsruhe, Report No. 86/70, 1970 (unpublished).

[8]R. W. Peelle and F. C. Maienschein, Phys. Rev. C 3, 373 (1971).

[9]V. V. Verbinski and R. E. Sund, Gulf General Atomic, DASA Report No. 2234, GA-9148, 1969 (to be published).

[10]H. Albinsson and L. Lindow, AB Atomenergi, Studsvik, Sweden, Report No. AE-398, 1970 (unpublished).

[11]H. Albinsson, AB Atomenergi, Studsvik, Sweden, Report No. AE-420, 1971 (unpublished).

[12]H. Albinsson, AB Atomenergi, Studsvik, Sweden, Report No. AE-417, 1971 (unpublished).

[13]P. Armbruster, H. Labus, and K. Reichelt, Z. Naturforsch. 26a, 512 (1971).

[14]H. Nifenecker, C. Signarbieux, M. Ribrag, J. Poitou, and J. Matuszek, to be published.

[15]H. Maier-Leibnitz, private communication.

[16]H. W. Schmitt and F. Pleasonton, Nucl. Instr. Methods 40, 204 (1966).

[17]H. W. Schmitt, W. M. Gibson, J. H. Neiler, F. J. Walter, and T. D. Thomas, in *Proceedings of the Symposium on the Physics and Chemistry of Fission, Salzburg, 1965* (See Ref. 1), Vol. I, p. 531.

[18]F. Plasil, R. L. Ferguson, F. Pleasonton, and H. W. Schmitt, to be published.

[19]Y. F. Apalin, Yu. N. Gritsyuk, I. E. Kutikov, V. I. Lebedev, and L. A. Mikaelyan, Nucl. Phys. 71, 553 (1965).

[20]H. W. Schmitt, J. H. Neiler, and F. J. Walter, Phys. Rev. 141, 1146 (1966).

[21]S. A. E. Johansson and P. Kleinheinz, in *Alpha-, Beta-, and Gamma-Ray Spectroscopy,* edited by K. Siegbahn (North-Holland, Amsterdam, 1966), Vol. I, p. 805.

[22]S. A. E. Johansson, Nucl. Phys. 60, 378 (1964).

[23]R. B. Leachman and C. S. Kazek, Phys. Rev. 105, 1511 (1957).

[24]J. Terrell, Phys. Rev. 127, 880 (1962).

[25]T. D. Thomas and J. R. Grover, Phys. Rev. 159, 980 (1967).

[26]M. M. Hoffman, Phys. Rev. 133, B714 (1964).

[27]F. Pleasonton, Oak Ridge National Laboratory Report No. ORNL-TM-3205, 1970 (unpublished), p. 14.

[28]F. E. W. Rau, Ann. Physik 10, 252 (1963).

[29]C. D. Zerby and H. S. Moran, Nucl. Instr. Methods 14, 115 (1961).

[30]International Atomic Energy Agency, Division of Research and Laboratories, Vienna, Set No. 248, Nov. 1970: ^{57}Co(0.122); ^{203}Hg(0.279); ^{22}Na(0.511, 1.275); ^{137}Cs(0.662); ^{54}Mn(0.835); ^{88}Y(0.898, 1.836) ^{60}Co(1.173, 1.332), where the numbers are the energies in units of MeV.

[31]J. L. Rodda, II, Oak Ridge National Laboratory Report No. ORNL-TM-2579, 1969 (unpublished).

[32]J. K. Bienlein and F. Pleasonton, Nucl. Phys. 68, 17 (1965).